EUROPEAN ORGANIZATION FOR NUCLEAR RESEARCH

CERN-PPE/95–14
February, 9 1995

Search for Neutralinos in Z Decays

The L3 Collaboration

Abstract

We have searched for neutralinos produced via the reactions $e^+e^- \rightarrow \chi\chi'$ and $e^+e^- \rightarrow \chi'\chi'$, where the next-to lightest neutralino, χ', decays into the lightest neutralino, χ, and either a photon or a fermion pair. Based on 1.8×10^6 hadronic Z decays collected with the L3 detector at LEP, no signal has been observed. We present upper limits of a few times 10^{-5} on the branching ratios $Z \rightarrow \chi\chi'$ and $Z \rightarrow \chi'\chi'$. In the framework of the Minimal Supersymmetric Standard Model, we exclude a lightest χ with m_χ less than 18 GeV, if either $\tan\beta > 2$ or the gluino mass $m_{\tilde{g}} > 100$ GeV.

accepted by Phys. Lett. B

Introduction

The Standard Model [1] has been very successful in describing data concerning electroweak interactions. However, it leaves many fundamental parameters unexplained such as the electroweak mixing parameter $\sin^2\theta_{\rm W}$. The quadratic divergences of scalar masses at the one–loop level and the large difference between the electroweak and grand unification scales (hierarchy problem) are further problems of the Standard Model. Supersymmetry (SUSY) addresses some of these questions. For every particle it predicts the existence of a partner particle with spin differing by half a unit. SUSY models in general require at least two higgs doublets. The partners of the $W^{\pm}$ and $H^{\pm}$ mix to form two mass eigenstates, the charginos $\widetilde{\chi}^{\pm}_{1,2}$. The partners of the γ, Z and the neutral higgs mix to form at least four mass eigenstates, the neutralinos [2] χ, χ', χ'' and χ''', in order of increasing mass.

In the Minimal Supersymmetric Standard Model (MSSM) [3], the Lagrangian at the unification scale is globally supersymmetric, except for a set of "soft breaking" mass terms. Among these are the gaugino masses M_1, M_2 and M_3 associated with the $U(1)_Y$, $SU(2)_L$ and $SU(3)_C$ gauge groups, respectively. These mass terms are assumed to be equal at the unification scale, leading to $M_1 = \frac{5}{3}M_2\tan^2\theta_W$ at the electroweak scale [4]. From naturalness arguments [5] it is expected that the gaugino mass parameter, M $\equiv M_2$, is in the range $0 \leq$M$\leq$ 250 GeV, the higgsino mass parameter, μ, is bounded by $0 \leq |\mu| \leq 200$ GeV and the ratio of the vacuum expectation values of the two higgs doublets, $\tan\beta = v_2/v_1$, is constrained to $1 \leq \tan\beta \leq \frac{m_t}{m_b} \sim 50$, where v_2 gives mass to quarks of charge $2/3e$ and v_1 gives mass to charged leptons and quarks of charge $-1/3e$. In the MSSM, the masses and interactions of the neutralinos and charginos are entirely described in terms of $\tan\beta$ and the two mass parameters M and μ. We will make the usual assumption that χ is the lightest supersymmetric particle (LSP), which is stable by R–parity conservation and escapes detection due to its weakly interacting nature.

Many experiments have looked for supersymmetric particles, but so far no signature has been found. There exist mass limits up to 45 GeV for most of the supersymmetric particles [6] except for neutralinos. The other LEP experiments derived lower mass limits of 20 GeV and 40 GeV for the two lightest neutralinos if $\tan\beta \geq 3$ and no limit for $\tan\beta < 1.6$. [7] The production cross section of neutralinos not only depends on their masses but also on their particle content and varies from almost 0, if one of the produced neutralinos is a photino, to several hundred picobarns. The analysis of a high statistics event sample, as presented here, is needed to derive conclusions.

We present the event selection and results of our search, which are based on 1.8×10^6 hadronic Z decays collected in 1991 — 1993. These results are interpreted in the MSSM context as well as in a more general way.

The L3 Detector

The L3 detector [8,9] covers 99% of the 4π solid angle. It consists of a central tracking chamber (TEC), a forward–backward tracking chamber, a high resolution electromagnetic calorimeter (ECAL) composed of Bismuth Germanium Oxide (BGO) crystals, a ring of scintillation counters, a uranium brass hadron calorimeter with proportional wire chambers (HCAL), and a high–precision muon chamber spectrometer (MUCH). These detectors are located in a 12 m diameter magnet providing a uniform field of 0.5 T along the beam direction. Forward BGO arrays (LUMI) on each side of the detector measure the luminosity by detecting the energy deposit of small angle Bhabha events.

Event Selection

We searched for neutralinos produced in the reaction

$$e^+e^- \longrightarrow \mathrm{Z} \longrightarrow \chi\chi' \text{ or } \chi'\chi'$$

with χ' decaying via

$$\chi' \longrightarrow \chi\mathrm{Z}^* \longrightarrow \chi f\bar{f} \qquad \text{or} \qquad \chi' \longrightarrow \chi\gamma.$$

The signature is missing energy due to the undetected χ and one or two photons, two or four acollinear and acoplanar leptons, or one to four hadronic jets from the primary quarks.

We assume that the masses of the lightest higgs, h^0 or A^0, and charginos, $\tilde{\chi}_1^\pm$, are sufficiently large [10] so that the decays $\chi' \rightarrow \chi\mathrm{h}^0, \chi\mathrm{A}^0$ and $\chi' \rightarrow \tilde{\chi}_1^\pm f\bar{f}'$ are kinematically forbidden. However, the signature of such decays would be very similar to $\chi' \rightarrow \chi\mathrm{Z}^* \rightarrow \chi\mathrm{q}\bar{\mathrm{q}}$ and could lead to even higher detection efficiencies. Because the SUSY partner of the electron, the selectron, is assumed to be heavier than 45 GeV [6], we neglect neutralino production via t-channel exchange, which is of the order of 10^{-3} relative to the s-channel contribution in the MSSM, if the neutralino is not a pure photino.

We used Monte Carlo generators to estimate the background arising from all Standard Model reactions. The main background sources for the fermionic neutralino decays are fermion pair production $\mathrm{e}^+\mathrm{e}^- \rightarrow \mathrm{q}\bar{\mathrm{q}}(\gamma)$ [12], $\mathrm{e}^+\mathrm{e}^- \rightarrow \tau^+\tau^-(\gamma)$ [13] and four-fermion processes $\mathrm{e}^+\mathrm{e}^- \rightarrow \mathrm{e}^+\mathrm{e}^- f\bar{f}$ [14]. The backgrounds for the radiative neutralino decays are $\mathrm{e}^+\mathrm{e}^- \rightarrow \nu\bar{\nu}\gamma$ [15] and $\mathrm{e}^+\mathrm{e}^- \rightarrow \gamma\gamma(\gamma)$ [16]. The detector response of the final state particles is simulated with the GEANT package using the GHEISHA program for hadronic interactions [17]. The simulated events are reconstructed and analyzed in the same way as the real data.

To determine the efficiency for neutralino detection, we have simulated the neutralino production and decay based on the formulae given in Reference 11. The detection efficiency for neutralinos depends on their masses, their relative CP–sign and their decay mode. A finite set of neutralino mass combinations was fully simulated as described above. To interpolate between these points in the m_χ–$m_{\chi'}$ mass plane, a fast simulation has been developed. Based on particle momenta, the detector response is evaluated taking detector (including trigger) efficiencies and resolutions into account. The agreement between the fast and full simulation is found to be better than 3%.

We have looked for the electroweak neutralino decay $\chi' \rightarrow \chi f\bar{f}$, where $f = \mathrm{q}, \mu, \mathrm{e}$ and for the radiative decay $\chi' \rightarrow \chi\gamma$. Due to the low visible energy and the small branching fraction, we did not investigate decays involving τ leptons.

Hadronic Final State

We select events with one or two jets in the final state, which may be interpreted as $\mathrm{Z} \rightarrow \chi\chi' \rightarrow \chi\chi\mathrm{q}\bar{\mathrm{q}}$, $\mathrm{Z} \rightarrow \chi'\chi' \rightarrow \chi\mathrm{q}\bar{\mathrm{q}}\chi\nu\bar{\nu}$, or $\mathrm{Z} \rightarrow \chi'\chi' \rightarrow \chi\mathrm{q}\bar{\mathrm{q}}\chi\mathrm{q}'\bar{\mathrm{q}}'$ events. Calorimetric jets are reconstructed using the Durham clustering algorithm [19] with $y_{cut} = 0.04$ and are required to have at least one associated TEC track. Depending on the kinematics of the reaction, the two initial decay quarks may be reconstructed as one or two jets. We did not study the three and four-jet topology, because of the large background arising from Standard Model $\mathrm{q}\bar{\mathrm{q}}(\mathrm{g})$ events. Also, their relative fraction compared to one and two-jet events was found to be small.
For hadronic one-jet events we require:

1. The jet to have at least 10 GeV transverse momentum in order to reject four-fermion background.

2. The event to contain at least 4 TEC tracks to remove single jets originating from one or three prong τ decays, where the other τ remains undetected.

3. There to be no TEC track in the r–ϕ plane in the hemisphere opposite to the jet direction, and the total calorimetric energy deposited in a cone of half opening angle of 30° around the missing energy direction to be less than 500 MeV. The contribution of most standard Z decays is therefore eliminated.

For hadronic two-jet events we require:

1. The acoplanarity and acollinearity angle of the two jets to exceed 40° to remove most standard Z decays (Fig. 1).

2. The total calorimetric energy deposited in a cone of half opening angle of 30° around the missing energy direction to be less than 500 MeV. There must be no TEC track within 30° of the missing energy direction in the r–ϕ plane. These requirements remove any remaining $q\bar{q}$ or $\tau^+\tau^-$ events.

3. We reduce the four-fermion background by requiring that the direction of the missing energy points more than 25° away from the beam axis, that each jet has at least 3 GeV transverse momentum and that no more than 10 GeV is deposited in the luminosity monitors.

No events survive the one-jet selection, while three events are left after applying the two-jet selection cuts consistent with an expected background from Standard Model four-fermion processes of 0.9 ± 0.4 events.[1)]

Muon Final State

In order to select candidates of the type $Z \to \chi\chi' \to \chi\chi\mu^+\mu^-$, one of the two muons must be identified in the muon chambers and the other one either in the muon chambers or as an isolated TEC track. We reject cosmic rays as described in [20]. Further selection criteria are:

1. The acoplanarity between the two muons has to exceed 40°, and the TEC track multiplicity has to be at most 2 to suppress the four-fermion background.

2. The most energetic ECAL or LUMI cluster should not exceed 2 GeV in order to remove radiative dimuons and four-fermion events respectively. This requirement also ensures that a muon candidate which is only identified by a TEC track corresponds to a real muon.

3. If both muons have been identified in the MUCH, the most energetic one has to have momentum $p > 6$ GeV. The missing transverse momentum of the event also has to exceed 6 GeV. In the case where one muon has been identified in the TEC, it should have a transverse momentum $p_T > 3$ GeV, while the other one (identified in the MUCH) should have $p > 10$ GeV. These cuts further reduce the four-fermion contribution.

No candidate events are observed after applying these cuts.

[1)]The cross section of the four-fermion Monte Carlo events has been normalized to fit the observed distributions in hadronic two-jet events.

Electron Final State

$Z \rightarrow \chi\chi' \rightarrow \chi\chi e^- e^+$ candidate events are selected by requiring at most three clusters in the ECAL. The two most energetic clusters are associated with a TEC track and must have more than 3 GeV and 2 GeV of energy. The energy of a possible third cluster has to be below 0.5 GeV. Furthermore:

1. The acoplanarity and acollinearity angle of the two most energetic clusters has to exceed 15° to reduce the four-fermion and Bhabha background.

2. The missing transverse momentum has to exceed 6 GeV and point more than 12° away from the beam axis and more than 5° away from the closest ECAL cluster to further reduce the $\tau^+\tau^-$ and four-fermion contamination.

3. The sum of the visible energy and missing momentum should not exceed the center-of-mass energy minus 5 GeV in order to suppress three-body final states with an undetected particle.

No events are left after applying these cuts.

Photon Final States

Photonic final states may result from the $\chi' \rightarrow \chi\gamma$ decay. They are selected by allowing up to three electromagnetic clusters in the ECAL and no other significant detector activity. The selection criteria are [21]:

1. The most energetic cluster in the LUMI should not exceed 5 GeV, while the most energetic cluster in the HCAL has to be below 3 GeV. This reduces the background from radiative Bhabha scattering.

2. Radiative cosmic muon and four-fermion backgrounds are removed by requiring no tracks in the TEC or MUCH.

3. Single-photon events are selected starting 20° away from the beam line. The transverse momentum of the photon has to exceed 10 GeV to suppress events from radiative neutrino production $\nu\bar{\nu}(\gamma)$ (Fig. 2).

4. Events with two photons are selected allowing for a third cluster. To suppress the Standard Model $\gamma\gamma(\gamma)$ final states, we require that the two most energetic photons have less than 40 GeV of energy each and an acoplanarity in excess of 3.5°. The missing transverse momentum has to be above 6 GeV.

No events survive the two-photon selection. 13 events survive in the one-photon sample, in good agreement with the Standard Model expectation from $\nu\bar{\nu}\gamma$ and $\gamma\gamma(\gamma)$ events of 15.7 ± 1.5.

Results

No excess over the Standard Model expectation has been observed (Table 1). The efficiency to detect neutralinos is high in the case where the χ–χ' mass difference is greater than 10 GeV (see Table 2 for details). It reaches 70% for the single-photon selection and up to 30% – 60%

Signature	Events	
	Observed	Expected
one jet	0	< 0.5
two jets	3	0.9 ± 0.4
two muons	0	< 0.5
two electrons	0	< 0.5
one photon	13	15.7 ± 1.5
two photons	0	0.7 ± 0.5

Table 1: The number of the observed events versus the number of expected background events for different neutralino decay channels.

particle mass		efficiency (%)					
$m_{\chi'}$ (GeV)	m_χ (GeV)	$\chi\chi q\bar{q}$	$\chi\chi e^+e^-$	$\chi\chi\mu^+\mu^-$	$\chi\chi\gamma$	$\chi q\bar{q}\chi(q'\bar{q}',\nu\bar{\nu})$	$\chi\gamma\chi\gamma$
5	0	25	50	42	50	9	37
10	5	35	50	40	43	12	43
30	0	36	51	50	60	15	61
30	25	8	24	17	9	4	14
45	0	36	53	50	71	10	67
45	35	9	30	23	20	7	53
55	0	32	51	47	73		
55	35	23	49	38	64		
75	0	27	45	41	76		
75	15	26	54	41	63		
90	0	27	26	43	76		

Table 2: Total neutralino detection efficiencies in percent. The quoted values correspond to the relative neutralino CP–sign with the lowest efficiency.

for signatures with hadronic jets, muons, electrons or two photons. The trigger efficiency for events passing all our cuts is more than 90% for most of the final state configurations.

In the absence of a neutralino signal, we set limits on the branching fractions $\mathrm{BR}(\mathrm{Z} \to \chi\chi')$ and $\mathrm{BR}(\mathrm{Z} \to \chi'\chi')$, which do not depend on the neutralino coupling constants. We subsequently interpret these results in the MSSM framework, excluding regions of the parameter space as well as establishing limits on the neutralino masses.

We present upper limits on the branching ratios $\mathrm{BR}(\mathrm{Z} \to \chi\chi', \chi'\chi')$ as a function of the neutralino masses, using the relative neutralino CP–sign that leads to the lowest detection efficiency. The branching ratios $\chi' \to \chi\mathrm{Z}^* \to \chi(e^+e^-, \mu^+\mu^-, q\bar{q}, \nu\bar{\nu})$ are calculated according to the Z partial width of these channels, while the neutralino decay width to photons is assumed to be unknown. We then vary the relative photonic branching ratio between 0 and 1 and quote the highest, most conservative, limit obtained. The different channels are combined to calculate limits on the $\mathrm{Z} \to \chi\chi'$ and $\mathrm{Z} \to \chi'\chi'$ decay modes taking the different branching ratios, detection efficiencies, numbers of candidates and expected background events properly into account using Poisson statistics in the Bayesian approach [22]. The 95% confidence level ($C.L.$) upper limits on $\mathrm{BR}(\mathrm{Z} \to \chi\chi')$ and $\mathrm{BR}(\mathrm{Z} \to \chi'\chi')$ are shown in Fig. 3 and 4.

Limits within the MSSM

In addition to the limits on $\mathrm{BR}(Z \to \chi\chi')$ and $\mathrm{BR}(Z \to \chi'\chi')$, we use the constraints coming from the precise LEP Z lineshape measurements[2)]

$$\begin{aligned}\Delta\Gamma_{\mathrm{Z}} &< 23.1 \text{ MeV } (95\%\ C.L.)\\ \Delta\Gamma_{inv} &< 8.4 \text{ MeV } (95\%\ C.L.)\end{aligned}$$

to restrict the MSSM parameter space using

$$\begin{aligned}\Delta\Gamma_{\mathrm{Z}} &= \Gamma(\mathrm{Z} \to \chi\chi) + \Gamma(\mathrm{Z} \to \chi\chi') + \Gamma(\mathrm{Z} \to \chi\chi'') + \\ &\quad \Gamma(\mathrm{Z} \to \chi\chi''') + \Gamma(\mathrm{Z} \to \chi'\chi') + \Gamma(\mathrm{Z} \to \tilde{\chi}_1^+\tilde{\chi}_1^-)\\ \Delta\Gamma_{inv} &= \Gamma(\mathrm{Z} \to \chi\chi).\end{aligned}$$

Changing the limits on $\Delta\Gamma_{\mathrm{Z}}$ and $\Delta\Gamma_{inv}$ by a factor of two does not change the excluded MSSM parameter space significantly. The excluded regions for different values of $\tan\beta$ are shown in Fig. 5. For moderate or high values of $\tan\beta$, a significant part of the accessible parameter space is excluded.

All neutralino masses are functions of the parameters M, μ and $\tan\beta$. Therefore, constraints on the MSSM parameter space translate into limits on these masses, summarized in Table 3. The dependence on $\tan\beta$ is illustrated in Fig. 6.

These neutralino mass limits can be further improved by using a limit on the gluino mass $m_{\tilde{g}} > 100$ GeV [24], as suggested by Hidaka [25], which limits the parameter M via

$$m_{\tilde{g}} = \frac{\alpha_s}{\alpha}\sin^2\theta_{\mathrm{W}}\mathrm{M} \qquad \text{thus} \qquad \mathrm{M} \approx 0.3 m_{\tilde{g}} > 30 \text{ GeV}.$$

This further restriction leads to mass limits for all $\tan\beta$ values, which are also shown in Table 3.

2)The limits on $\Delta\Gamma_{\mathrm{Z}}$ and $\Delta\Gamma_{inv}$ are obtained with the method described in [9] using the results given by [23]. We have used $m_{\mathrm{H}^0} = 1000$ GeV, $m_{\mathrm{t}} = 131$ GeV, $\alpha_{\mathrm{s}} = 0.117$, $m_{\mathrm{Z}} = 91.180$ GeV, $\Gamma_{\mathrm{Z}} = 2490 \pm 7$ MeV and $\Gamma_{inv} = 498.2 \pm 4.2$ MeV, which are the values that give the most conservative constraints.

Particle	$\tan\beta > 1$	$\tan\beta > 2$	$\tan\beta > 3$	$m_{\tilde{g}} > 100$ GeV all $\tan\beta$
χ	0 GeV	20 GeV	23 GeV	18 GeV
χ'	0 GeV	46 GeV	52 GeV	20 GeV
χ''	60 GeV	78 GeV	84 GeV	60 GeV
χ'''	90 GeV	115 GeV	127 GeV	98 GeV

Table 3: Lower neutralino mass limits (95% $C.L.$)

Conclusion

Using the 1991–1993 data of the L3 experiment, we have searched for neutralinos with a large variety of event signatures. No evidence for neutralinos was found and upper limits of a few times 10^{-5} have been set on the branching ratio for Z decaying to $\chi\chi'$ or $\chi'\chi'$. A significant part of the MSSM parameter space accessible at LEP has been excluded. In this paper the branching ratio limits are significantly improved compared to earlier results [7] and the dependence on assumptions on the neutralino decay modes has been minimized. In the MSSM the lightest neutralino is found to be heavier than 18 GeV, if either $\tan\beta > 2$ or $m_{\tilde{g}} > 100$ GeV.

Acknowledgments

We wish to express our gratitude to the CERN accelerator division for the excellent performance of the LEP machine. We acknowledge the efforts of all engineers and technicians who have participated in the construction and maintenance of this experiment.

References

[1] S.L. Glashow, Nucl. Phys. 22 (1961) 579;
S. Weinberg, Phys. Rev. Lett. 19 (1967) 1264;
A. Salam, Elementary Particle Theory, Ed. N. Svartholm, Stockholm, "Almquist and Wiksell" (1968) 367.

[2] R. Barbieri et. al. , Z Physics at LEP1, CERN 89-08 (1989) Vol. 2,121;
J. M. Frere, G. L. Kane, Nucl. Phys. B223 (1983) 331;
J. Ellis et al., Phys. Lett. B127 (1983) 233;
G. Gamberini, Z. Phys., C30 (1986) 605;
J. Ellis et al., Phys. Lett. B123 (1983) 436.

[3] Y.A. Goldfand and E.P. Likhtman, JETP Lett. 13 (1971) 323;
D.V. Volkhov and V.P. Akulov, Phys. Lett. B46 (1973) 109;
J. Wess and B. Zumino, Nucl. Phys. B70 (1974) 39;
P. Fayet and S. Ferrara, Phys. Rep. 32 (1977) 249;
A. Salam and J. Strathdee, Fortschr. Phys. 26 (1978) 57.

[4] For reviews, see H. Nilles, Phys. Rep. 110 (1984) 1;
R. Barbieri, Riv. Nuovo Cimento 11, No. 4 (1988);
R. Barbieri et al., Nucl. Phys. B296 (1988) 75.

[5] J. Ellis et al., Mod. Phys. Lett. A1 (1986) 57;
R. Barbieri and G.F. Giudice, Nucl. Phys. B306 (1988) 63;
Z. Kunszt and F. Zwirner, CERN–TH.6150/91, ETH-TH/91-7, Dec. 91.

[6] J. Ellis et al., CERN-PPE/92-180

[7] ALEPH Collab., D. Decamp et al., Phys. Lett. B244 (1990) 541;
ALEPH Collab., D. Decamp et al., Phys. Rep. 216 (1992) 253;
DELPHI Collab., P. Abreu et al., Phys. Lett. B247 (1990) 157;
OPAL Collab., M.Z. Akrawy et al., Phys. Lett. B248 (1990) 211.

[8] L3 Collab., B. Adeva et al., NIM A289 (1990) 35

[9] L3 Collab., O. Adriani et al., Phys. Rep. 236 (1993) 1

[10] ALEPH Collab., D. Decamp et al., Phys. Lett. B236 (1990) 86;
ALEPH Collab., D. Decamp et al., Phys. Lett. B237 (1990) 291.

[11] A. Bartl, H. Fraas and W. Majerotto, Nucl. Phys. B278 (1986) 1;
H.E. Haber and D. Wyler, Nucl. Phys. B323 (1989) 267.

[12] JETSET 7.3: T. Sjöstrand, M. Bengtsson, Comput. Phys. Commun. 43 (1987) 367;
M. Böhm, A. Denner and W. Hollik, Nucl. Phys. B304 (1988) 687.

[13] KORALZ: S. Jadach et al., "Z Physics at LEP 1", eds. G. Altarelli et al., CERN Report CERN-89-08, Vol. 3(1989)

[14] DIAG 36: F.A. Berends et al., Nucl. Phys. B253 (1985) 441

[15] R. Miquel et al., Z. Phys. C48 (1990) 309;
F.A. Berends et al., Nucl. Phys. B301 (1988) 583.

[16] F.A. Berends, R. Kleiss, Nucl. Phys. B186 (1981) 22

[17] GEANT 3.15: R. Brun et al., CERN-DD/78-2;
GHEISHA: H. Fesefeld, RWTH Aachen Preprint PITHA 85/02 (1985).

[18] P. Béné et al., NIM A306 (1991) 150;
R. Bizzarri et al., NIM A317 (1992) 463;
P. Bagnaia et al., NIM A324 (1993) 101.

[19] S. Bethke et al., Nucl. Phys. B370 (1992) 310

[20] L3 Collab., O. Adriani et al., Z. Phys. C62 (1994) 551

[21] See A. Weber, Thesis, RWTH Aachen Preprint PITHA 94/18 (1994) for further details.

[22] A.G. Frodesen, O. Skjeggestad, H. Töfte, Probability and statistics in Particle Physics, (Universitetforlaget, Bergen – 1979).

[23] Review of Particle Properties, L. Montanet et al., Phys. Rev. D50 (1994) 1173

[24] CDF Collab., F. Abe et al., Phys. Rev. Lett. 69 (1992) 3439;
H. Baer, X. Tataand J. Woodside, Phys. Rev. D44 (1991) 207.

[25] K. Hidaka, Phys. Rev. D44 (1991) 927;
I. Antoniadis, J. Ellis and D.V. Nanopoulos, Phys. Lett. B262 (1991) 109

The L3 Collaboration:

M.Acciarri,[26] A.Adam,[43] O.Adriani,[16] M.Aguilar-Benitez,[25] S.Ahlen,[10] B.Alpat,[33] J.Alcaraz,[25] J.Allaby,[17] A.Aloisio,[28] G.Alverson,[11] M.G.Alviggi,[28] G.Ambrosi,[33] Q.An,[18] H.Anderhub,[46] A.L.Anderson,[15] V.P.Andreev,[37] T.Angelescu,[12] D.Antreasyan,[8] A.Arefiev,[27] T.Azemoon,[3] T.Aziz,[9] P.V.K.S.Baba,[18] P.Bagnaia,[36,17] J.A.Bakken,[35] L.Baksay,[42] R.C.Ball,[3] S.Banerjee,[9] K.Banicz,[43] R.Barillère,[17] L.Barone,[36] P.Bartalini,[33] A.Baschirotto,[26] M.Basile,[8] R.Battiston,[33] A.Bay,[22] F.Becattini,[16] U.Becker,[15] F.Behner,[46] Gy.L.Bencze,[13] J.Berdugo,[25] P.Berges,[15] B.Bertucci,[17] B.L.Betev,[46] M.Biasini,[33] A.Biland,[46] G.M.Bilei[33] R.Bizzarri,[36] J.J.Blaising,[17] G.J.Bobbink,[2] R.Bock,[1] A.Böhm,[1] B.Borgia,[36] A.Boucham,[4] D.Bourilkov,[46] M.Bourquin,[19] D.Boutigny,[4] B.Bouwens,[2] E.Brambilla,[15] J.G.Branson,[38] V.Brigljevic,[46] I.C.Brock,[34] A.Bujak,[43] J.D.Burger,[15] W.J.Burger,[19] C.Burgos,[25] J.Busenitz,[42] A.Buytenhuijs,[30] X.D.Cai,[18] M.Capell,[15] G.Cara Romeo,[8] M.Caria,[33] G.Carlino,[28] A.M.Cartacci,[16] J.Casaus,[25] G.Castellini,[16] R.Castello,[26] N.Cavallo,[28] C.Cecchi,[19] M.Cerrada,[25] F.Cesaroni,[36] M.Chamizo,[25] Y.H.Chang,[48] U.K.Chaturvedi,[18] M.Chemarin,[24] A.Chen,[48] C.Chen,[6] G.Chen,[6] G.M.Chen,[6] H.F.Chen,[20] H.S.Chen,[6] M.Chen,[15] G.Chiefari,[28] C.Y.Chien,[5] M.T.Choi,[41] S.Chung,[15] L.Cifarelli,[8] F.Cindolo,[8] C.Civinini,[16] I.Clare,[15] R.Clare,[15] T.E.Coan,[23] H.O.Cohn,[31] G.Coignet,[4] N.Colino,[17] V.Commichau,[1] S.Costantini,[36] F.Cotorobai,[12] B.de la Cruz,[25] X.T.Cui,[18] X.Y.Cui,[18] T.S.Dai,[15] R.D'Alessandro,[16] R.de Asmundis,[28] H.De Boeck,[30] A.Degré,[4] K.Deiters,[44] E.Dénes,[13] P.Denes,[35] F.DeNotaristefani,[36] D.DiBitonto,[42] M.Diemoz,[36] C.Dionisi,[36] M.Dittmar,[46] A.Doria,[28] I.Dorne,[4] M.T.Dova,[18,♯] E.Drago,[28] D.Duchesneau,[17] F.Duhem,[4] P.Duinker,[2] I.Duran,[39] S.Dutta,[9] S.Easo,[33] H.El Mamouni,[24] A.Engler,[34] F.J.Eppling,[15] F.C.Erné,[2] J.P.Ernenwein,[24] P.Extermann,[19] R.Fabbretti,[44] M.Fabre,[44] R.Faccini,[36] S.Falciano,[36] A.Favara,[16] J.Fay,[24] M.Felcini,[46] T.Ferguson,[34] D.Fernandez,[25] G.Fernandez,[25] F.Ferroni,[36] H.Fesefeldt,[1] E.Fiandrini,[33] J.H.Field,[19] F.Filthaut,[34] P.H.Fisher,[5] G.Forconi,[15] L.Fredj,[19] K.Freudenreich,[46] M.Gailloud,[22] Yu.Galaktionov,[27,15] S.N.Ganguli,[9] P.Garcia-Abia,[25] S.S.Gau,[11] S.Gentile,[36] J.Gerald,[5] N.Gheordanescu,[12] S.Giagu,[36] S.Goldfarb,[22] J.Goldstein,[10] Z.F.Gong,[20] E.Gonzalez,[25] A.Gougas,[5] D.Goujon,[19] G.Gratta,[32] M.W.Gruenewald,[7] C.Gu,[18] M.Guanziroli,[18] V.K.Gupta,[35] A.Gurtu,[9] H.R.Gustafson,[3] L.J.Gutay,[43] B.Hartmann,[1] A.Hasan,[29] J.T.He,[6] T.Hebbeker,[7] M.Hebert,[38] A.Hervé,[17] K.Hilgers,[1] W.C.van Hoek,[30] H.Hofer,[46] H.Hoorani,[19] S.R.Hou,[48] G.Hu,[18] M.M.Ilyas,[18] V.Innocente,[17] H.Janssen,[4] B.N.Jin,[6] L.W.Jones,[3] P.de Jong,[15] I.Josa-Mutuberria,[25] A.Kasser,[22] R.A.Khan,[18] Yu.Kamyshkov,[31] P.Kapinos,[45] J.S.Kapustinsky,[23] Y.Karyotakis,[4] M.Kaur,[18] S.Khokhar,[18] M.N.Kienzle-Focacci,[19] D.Kim,[5] J.K.Kim,[41] S.C.Kim,[41] Y.G.Kim,[41] W.W.Kinnison,[23] A.Kirkby,[32] D.Kirkby,[32] J.Kirkby,[17] S.Kirsch,[45] W.Kittel,[30] A.Klimentov,[15,27] A.C.König,[30] E.Koffeman,[2] O.Kornadt,[1] V.Koutsenko,[15,27] A.Koulbardis,[37] R.W.Kraemer,[34] T.Kramer,[15] W.Krenz,[1] H.Kuijten,[30] A.Kunin,[15,27] P.Ladron de Guevara,[25] G.Landi,[16] M.Lanfranchi,[33] S.Lanzano,[28 †] K.Lassila-Perini,[46] P.Laurikainen,[21] M.Lebeau,[17] A.Lebedev,[15] P.Lebrun,[24] P.Lecomte,[46] J.Lecoq,[4] P.Lecoq,[17] P.Le Coultre,[46] J.S.Lee,[41] K.Y.Lee,[41] I.Leedom,[11] C.Leggett,[3] J.M.Le Goff,[17] R.Leiste,[45] M.Lenti,[16] E.Leonardi,[36] P.Levtchenko,[37] C.Li,[20,18] E.Lieb,[45] W.T.Lin,[48] F.L.Linde,[2] B.Lindemann,[1] L.Lista,[28] Y.Liu,[18] Z.A.Liu,[6] W.Lohmann,[45] E.Longo,[36] W.Lu,[32] Y.S.Lu,[6] K.Lübelsmeyer,[1] C.Luci,[36] D.Luckey,[15] L.Ludovici,[36] L.Luminari,[36] W.Lustermann,[44] W.G.Ma,[20] A.Macchiolo,[16] M.Maity,[9] L.Malgeri,[36] R.Malik,[18] A.Malinin,[27] C.Maña,[25] S.Mangla,[9] M.Maolinbay,[46] P.Marchesini,[46] A.Marin,[10] J.P.Martin,[24] F.Marzano,[36] G.G.G.Massaro,[2] K.Mazumdar,[9] T.McMahon,[43] D.McNally,[17] S.Mele,[28] M.Merk,[34] L.Merola,[28] M.Meschini,[16] W.J.Metzger,[30] Y.Mi,[22] A.Mihul,[12] A.J.W.van Mil,[30] Y.Mir,[18] G.Mirabelli,[36] J.Mnich,[17] M.Möller,[1] V.Monaco,[36] B.Monteleoni,[16] R.Moore,[3] R.Morand,[4] S.Morganti,[36] N.E.Moulai,[18] R.Mount,[32] S.Müller,[1] E.Nagy,[13] M.Napolitano,[28] F.Nessi-Tedaldi,[46] H.Newman,[32] M.A.Niaz,[18] A.Nippe,[1] H.Nowak,[45] G.Organtini,[36] R.Ostonen,[21] D.Pandoulas,[1] S.Paoletti,[36] P.Paolucci,[28] G.Pascale,[36] G.Passaleva,[16] S.Patricelli,[28] T.Paul,[33] M.Pauluzzi,[33] C.Paus,[1] F.Pauss,[46] Y.J.Pei,[1] S.Pensotti,[26] D.Perret-Gallix,[4] A.Pevsner,[5] D.Piccolo,[28] M.Pieri,[16] J.C.Pinto,[34] P.A.Piroué,[35] E.Pistolesi,[16] F.Plasil,[31] V.Plyaskin,[27] M.Pohl,[46] V.Pojidaev,[27,16] H.Postema,[15] N.Produit,[19] K.N.Qureshi,[18] R.Raghavan,[9] G.Rahal-Callot,[46] P.G.Rancoita,[26] M.Rattaggi,[26] G.Raven,[2] P.Razis,[29] K.Read,[31] M.Redaelli,[26] D.Ren,[46] Z.Ren,[18] M.Rescigno,[36] S.Reucroft,[11] A.Ricker,[1] S.Riemann,[45] B.C.Riemers,[43] K.Riles,[3] O.Rind,[3] H.A.Rizvi,[18] S.Ro,[41] A.Robohm,[46] F.J.Rodriguez,[25] B.P.Roe,[3] M.Röhner,[1] S.Röhner,[1] L.Romero,[25] S.Rosier-Lees,[4] Ph.Rosselet,[22] W.van Rossum,[2] S.Roth,[1] J.A.Rubio,[17] H.Rykaczewski,[46] J.Salicio,[17] J.M.Salicio,[25] E.Sanchez,[25] A.Santocchia,[33] M.E.Sarakinos,[43] S.Sarkar,[9] G.Sartorelli,[18] M.Sassowsky,[1] G.Sauvage,[4] C.Schäfer,[1] V.Schegelsky,[37] D.Schmitz,[1] P.Schmitz,[1] M.Schneegans,[4] B.Schoeneich,[45] N.Scholz,[46] H.Schopper,[47] D.J.Schotanus,[30] R.Schulte,[1] K.Schultze,[1] J.Schwenke,[1] G.Schwering,[1] C.Sciacca,[28] R.Sehgal,[18] P.G.Seiler,[44] J.C.Sens,[48] L.Servoli,[33] I.Sheer,[38] S.Shevchenko,[32] N.Shivarov,[40] S.Shotkin,[15] V.Shoutko,[27] J.Shukla,[23] E.Shumilov,[27] D.Son,[41] A.Sopczak,[17] V.Soulimov,[28] C.Spartiotis,[21] T.Spickermann,[1] P.Spillantini,[16] M.Steuer,[15] D.P.Stickland,[35] F.Sticozzi,[15] H.Stone,[35] B.Stoyanov,[40] K.Strauch,[14] K.Sudhakar,[9] G.Sultanov,[18] L.Z.Sun,[20,18] G.F.Susinno,[19] H.Suter,[46] J.D.Swain,[18] A.A.Syed,[30] X.W.Tang,[6] L.Taylor,[11] R.Timellini,[8] Samuel C.C.Ting,[15] S.M.Ting,[15] O.Toker,[33] M.Tonutti,[1] S.C.Tonwar,[9] J.Tóth,[13] A.Tsaregorodtsev,[37] G.Tsipolitis,[34] C.Tully,[35] H.Tuchscherer,[42] J.Ulbricht,[46] L.Urbán,[13] U.Uwer,[1] E.Valente,[36] R.T.Van de Walle,[30] I.Vetlitsky,[27] G.Viertel,[46] P.Vikas,[18] U.Vikas,[18] M.Vivargent,[4] R.Voelkert,[45] H.Vogel,[34] H.Vogt,[45] I.Vorobiev,[27] A.A.Vorobyov,[37] An.A.Vorobyov,[37] L.Vuilleumier,[22] M.Wadhwa,[25] W.Wallraff,[1] J.C.Wang,[15] X.L.Wang,[20] Y.F.Wang,[15] Z.M.Wang,[18,20] A.Weber,[1] R.Weill,[22] C.Willmott,[25] F.Wittgenstein,[17] D.Wright,[35] S.X.Wu,[18] S.Wynhoff,[1] J.Xu,[10] Z.Z.Xu,[20] B.Z.Yang,[20] C.G.Yang,[6] G.Yang,[18] X.Y.Yao,[6] C.H.Ye,[18] J.B.Ye,[20] Q.Ye,[18] S.C.Yeh,[48] J.M.You,[34] N.Yunus,[18] M.Yzerman,[2] C.Zaccardelli,[32] An.Zalite,[37] P.Zemp,[46] J.Y.Zeng,[6] M.Zeng,[18] Y.Zeng,[1] Z.Zhang,[6] Z.P.Zhang,[20,18] B.Zhou,[10] G.J.Zhou,[6] J.F.Zhou,[1] Y.Zhou,[3] G.Y.Zhu,[6] R.Y.Zhu,[32] A.Zichichi,[8,17,18] B.C.C.van der Zwaan.[2]

1 I. Physikalisches Institut, RWTH, D-52056 Aachen, FRG[§]
III. Physikalisches Institut, RWTH, D-52056 Aachen, FRG[§]
2 National Institute for High Energy Physics, NIKHEF, NL-1009 DB Amsterdam, The Netherlands
3 University of Michigan, Ann Arbor, MI 48109, USA
4 Laboratoire d'Annecy-le-Vieux de Physique des Particules, LAPP,IN2P3-CNRS, BP 110, F-74941 Annecy-le-Vieux CEDEX, France
5 Johns Hopkins University, Baltimore, MD 21218, USA
6 Institute of High Energy Physics, IHEP, 100039 Beijing, China
7 Humboldt University, D-10099 Berlin, FRG[§]
8 INFN-Sezione di Bologna, I-40126 Bologna, Italy
9 Tata Institute of Fundamental Research, Bombay 400 005, India
10 Boston University, Boston, MA 02215, USA
11 Northeastern University, Boston, MA 02115, USA
12 Institute of Atomic Physics and University of Bucharest, R-76900 Bucharest, Romania
13 Central Research Institute for Physics of the Hungarian Academy of Sciences, H-1525 Budapest 114, Hungary[‡]
14 Harvard University, Cambridge, MA 02139, USA
15 Massachusetts Institute of Technology, Cambridge, MA 02139, USA
16 INFN Sezione di Firenze and University of Florence, I-50125 Florence, Italy
17 European Laboratory for Particle Physics, CERN, CH-1211 Geneva 23, Switzerland
18 World Laboratory, FBLJA Project, CH-1211 Geneva 23, Switzerland
19 University of Geneva, CH-1211 Geneva 4, Switzerland
20 Chinese University of Science and Technology, USTC, Hefei, Anhui 230 029, China
21 SEFT, Research Institute for High Energy Physics, P.O. Box 9, SF-00014 Helsinki, Finland
22 University of Lausanne, CH-1015 Lausanne, Switzerland
23 Los Alamos National Laboratory, Los Alamos, NM 87544, USA
24 Institut de Physique Nucléaire de Lyon, IN2P3-CNRS,Université Claude Bernard, F-69622 Villeurbanne Cedex, France
25 Centro de Investigaciones Energeticas, Medioambientales y Tecnologicas, CIEMAT, E-28040 Madrid, Spain♭
26 INFN-Sezione di Milano, I-20133 Milan, Italy
27 Institute of Theoretical and Experimental Physics, ITEP, Moscow, Russia
28 INFN-Sezione di Napoli and University of Naples, I-80125 Naples, Italy
29 Department of Natural Sciences, University of Cyprus, Nicosia, Cyprus
30 University of Nymegen and NIKHEF, NL-6525 ED Nymegen, The Netherlands
31 Oak Ridge National Laboratory, Oak Ridge, TN 37831, USA
32 California Institute of Technology, Pasadena, CA 91125, USA
33 INFN-Sezione di Perugia and Universitá Degli Studi di Perugia, I-06100 Perugia, Italy
34 Carnegie Mellon University, Pittsburgh, PA 15213, USA
35 Princeton University, Princeton, NJ 08544, USA
36 INFN-Sezione di Roma and University of Rome, "La Sapienza", I-00185 Rome, Italy
37 Nuclear Physics Institute, St. Petersburg, Russia
38 University of California, San Diego, CA 92093, USA
39 Dept. de Fisica de Particulas Elementales, Univ. de Santiago, E-15706 Santiago de Compostela, Spain
40 Bulgarian Academy of Sciences, Central Laboratory of Mechatronics and Instrumentation, BU-1113 Sofia, Bulgaria
41 Center for High Energy Physics, Korea Advanced Inst. of Sciences and Technology, 305-701 Taejon, Republic of Korea
42 University of Alabama, Tuscaloosa, AL 35486, USA
43 Purdue University, West Lafayette, IN 47907, USA
44 Paul Scherrer Institut, PSI, CH-5232 Villigen, Switzerland
45 DESY-Institut für Hochenergiephysik, D-15738 Zeuthen, FRG
46 Eidgenössische Technische Hochschule, ETH Zürich, CH-8093 Zürich, Switzerland
47 University of Hamburg, D-22761 Hamburg, FRG
48 High Energy Physics Group, Taiwan, China
§ Supported by the German Bundesministerium für Bildung, Wissenschaft, Forschung und Technologie
‡ Supported by the Hungarian OTKA fund under contract number 2970.
♭ Supported also by the Comisión Interministerial de Ciencia y Technología
♯ Also supported by CONICET and Universidad Nacional de La Plata, CC 67, 1900 La Plata, Argentina
† Deceased.

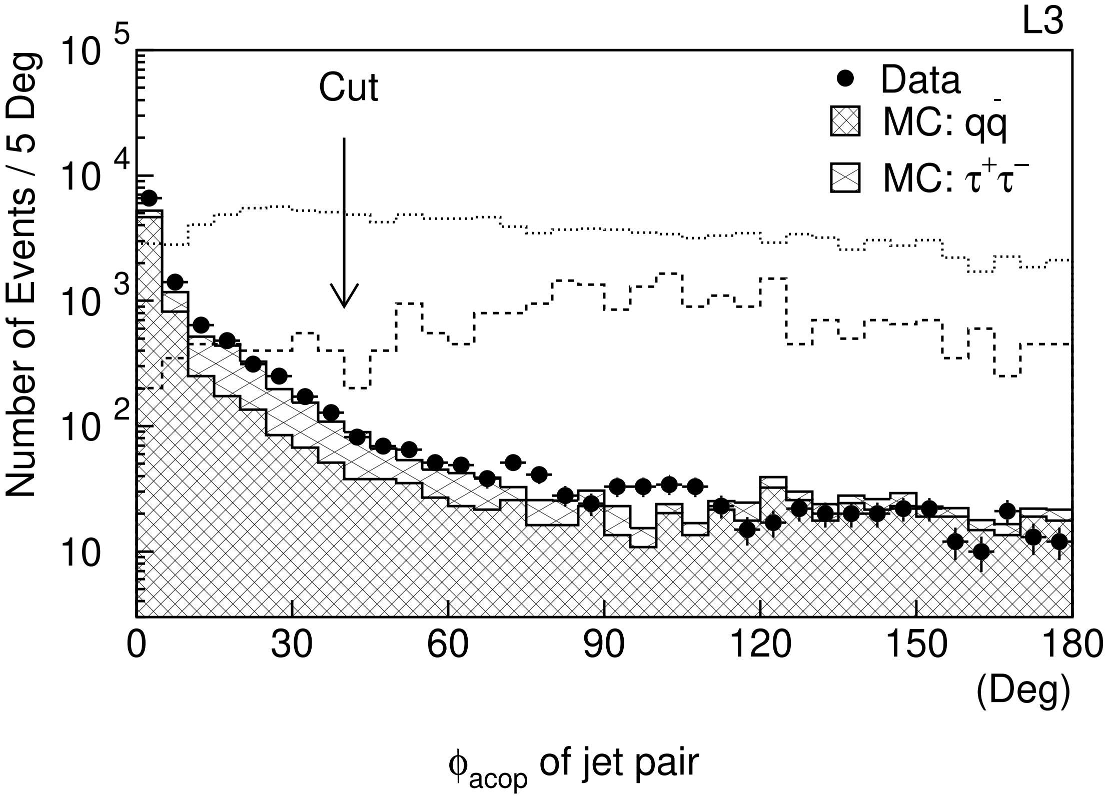

Figure 1: Acoplanarity distribution of the hadronic two-jet events. The points correspond to the data, while the solid lines indicate the results of the Standard Model Monte Carlo simulation (MC). The dotted line shows a possible signal for $\chi - \chi'$ production with neutralinos of mass $m_\chi = 0$ GeV and $m_{\chi'} = 85$ GeV and a 2.5 nanobarn cross section of production, while the dashed line corresponds to $m_\chi = 35$ GeV, $m_{\chi'} = 50$ GeV and a 0.5 nanobarn cross section.

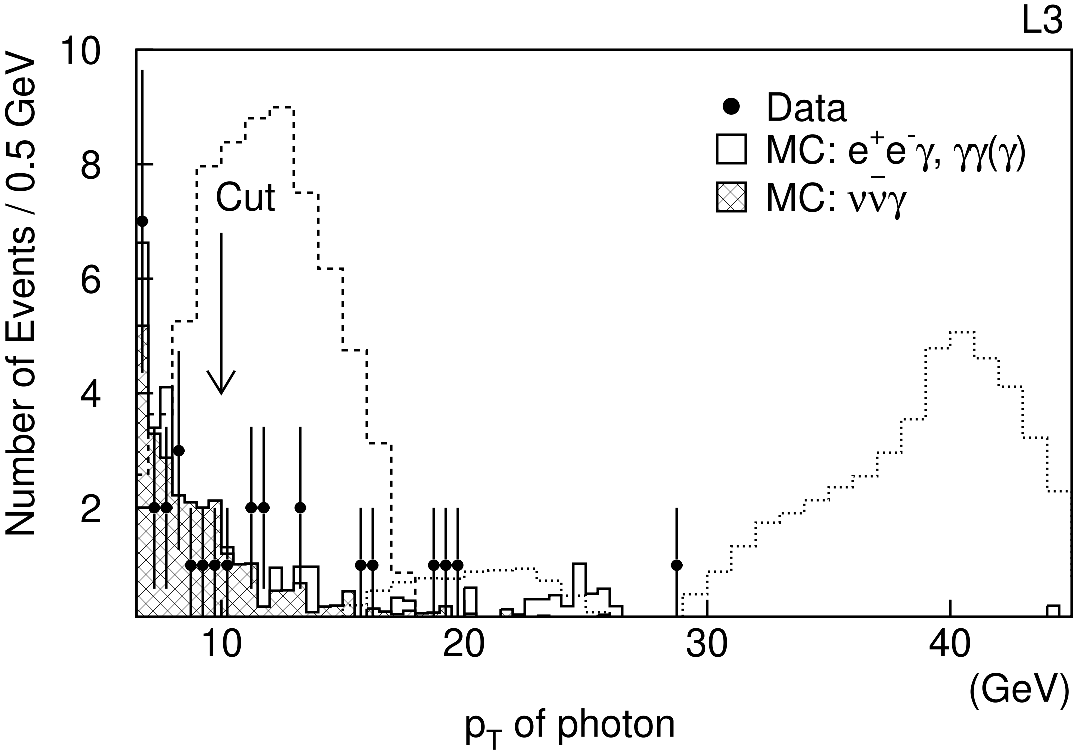

Figure 2: Transverse momentum distribution of the single-photon events. The points correspond to the data, while the solid lines indicate the results of a Standard Model Monte Carlo simulation (MC). The dotted line shows a possible signal for $\chi - \chi'$ production with neutralinos of mass $m_\chi = 0$ GeV and $m_{\chi'} = 85$ GeV and a 1.2 picobarn production cross section, while the dashed line corresponds to $m_\chi = 35$ GeV, $m_{\chi'} = 50$ GeV and a 1.6 picobarn cross section.

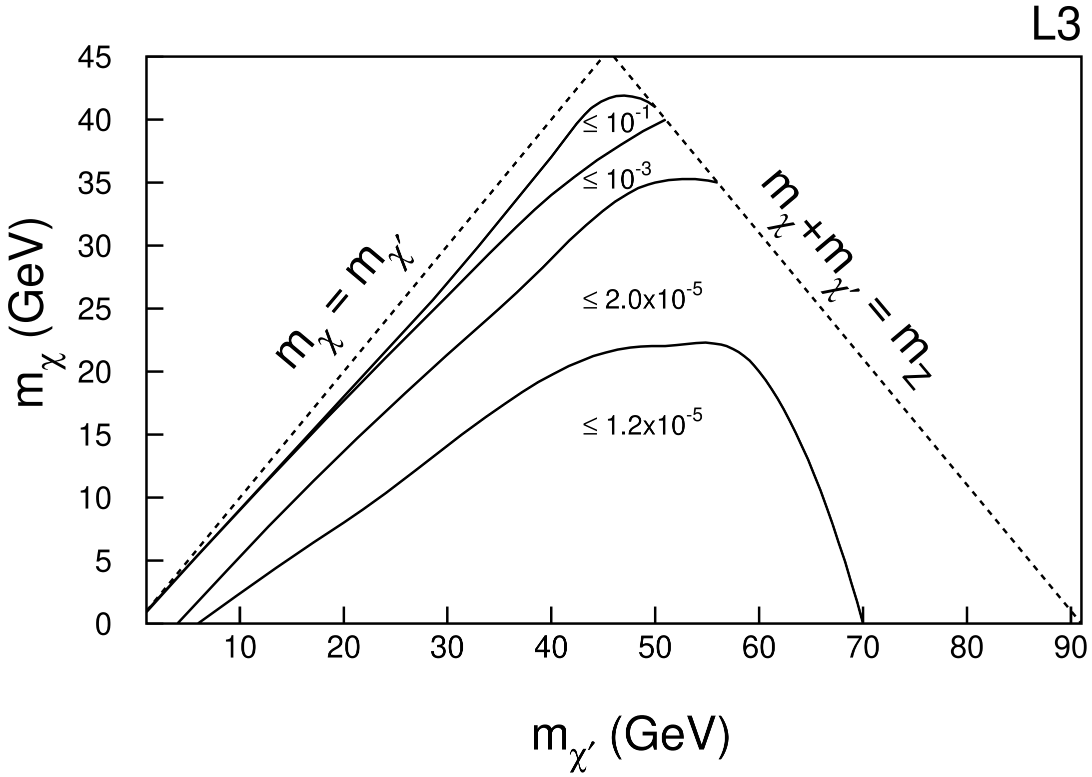

Figure 3: Contour plot of the 95% $C.L.$ upper limits on $Br(\mathrm{Z} \rightarrow \chi\chi')$ versus the χ and χ' masses. The solid lines separate the regions, where the limit on the branching ratio is smaller than the value shown, while the dashed lines show the kinematical limits of the channel.

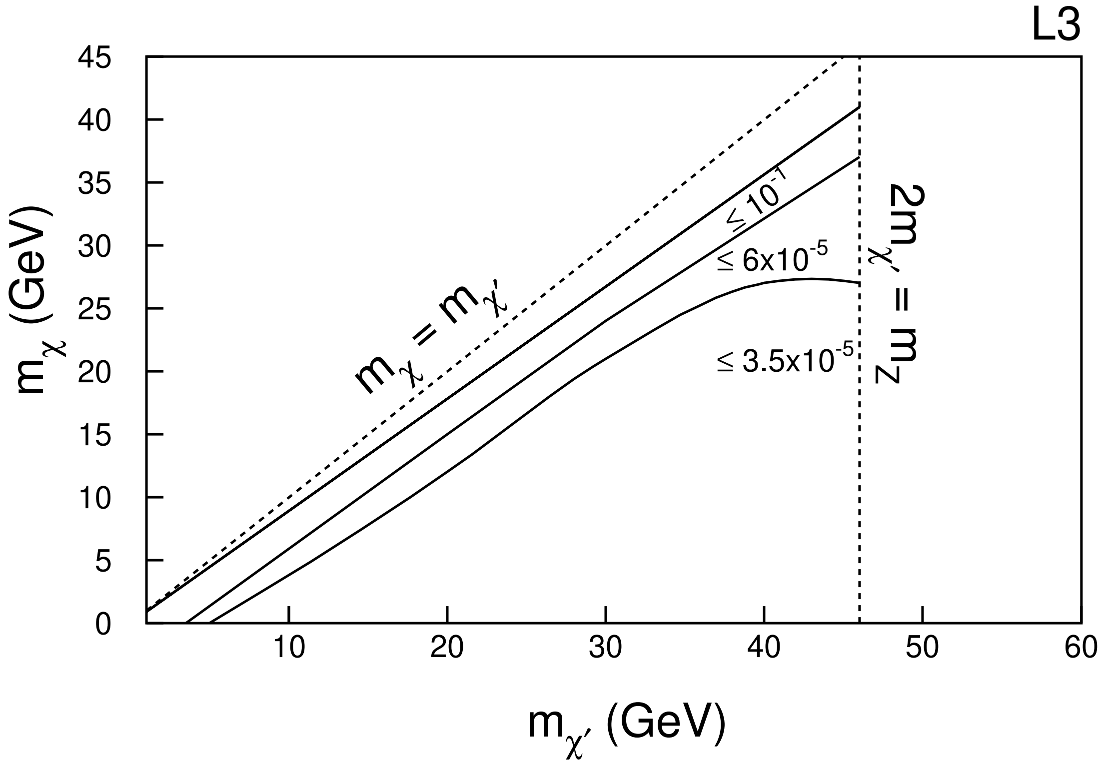

Figure 4: Contour plot of the 95% $C.L.$ upper limits on $Br(\mathrm{Z} \rightarrow \chi'\chi')$ versus the χ and χ' masses. The solid lines separate the regions, where the limit on the branching ration is smaller than the value shown, while the dashed lines show the kinematical limits of the channel.

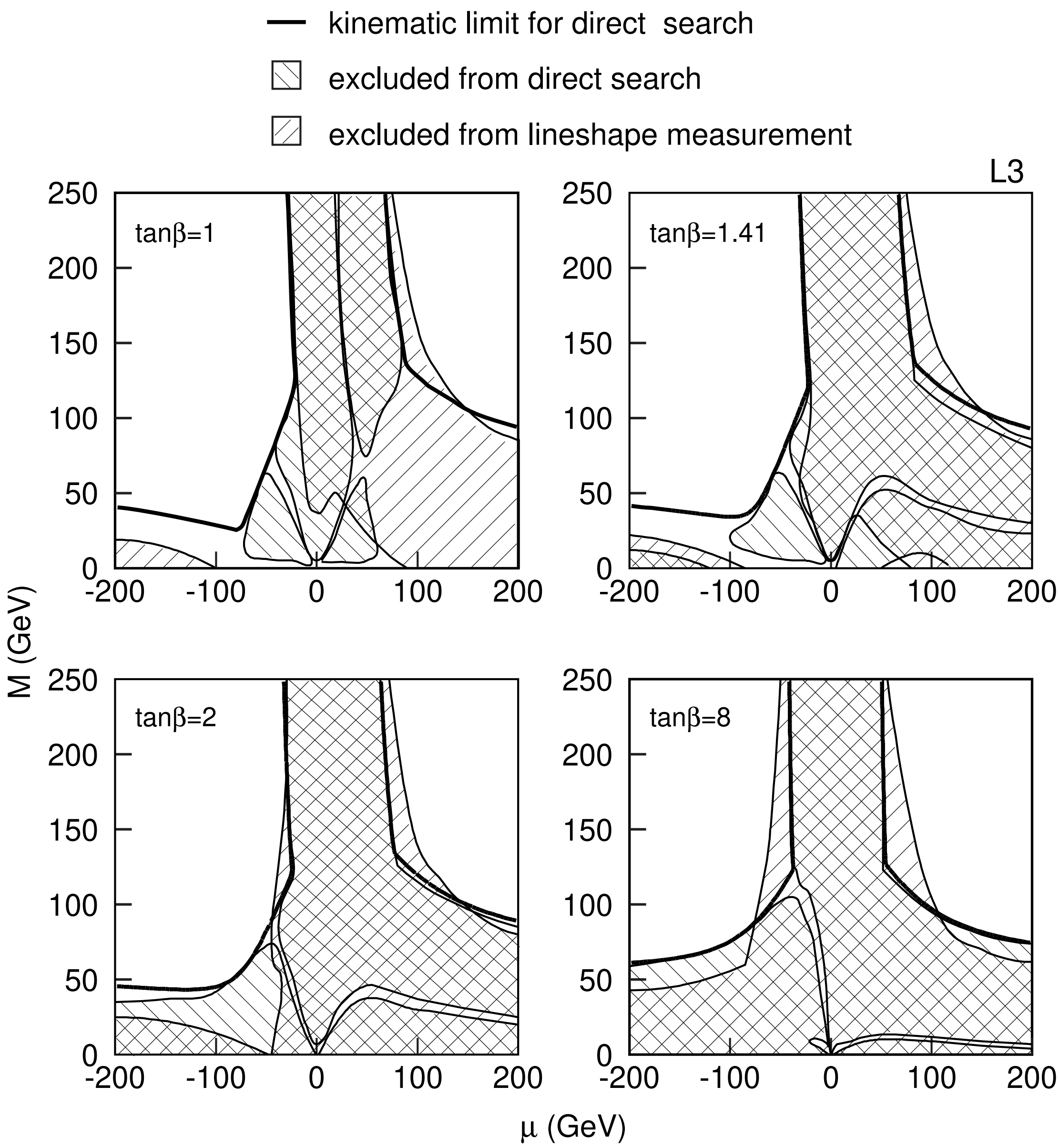

Figure 5: The excluded regions of the MSSM parameter space at the 95% *C.L.* as a function of the parameters M and μ. The kinematical limit corresponds to the the sum of the lightest and next to lightest neutralino masses being equal to the center-of-mass energy. The exclusion coming from the lineshape measurement goes beyond the kinematic limit of the direct search.

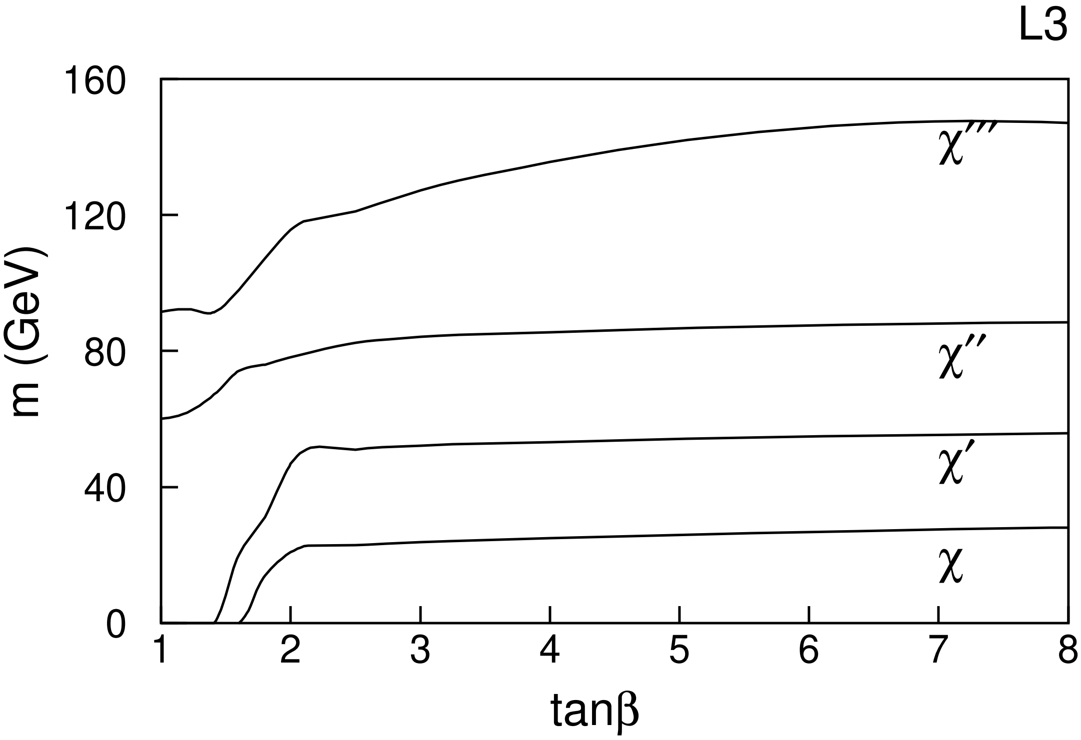

Figure 6: Neutralino lower mass limits (95% $C.L.$). The lines correspond to the lower mass limit for the different neutralinos. The regions below the lines are excluded.